J Ginseng Res 44 (2020) 350–361

Contents lists available at ScienceDirect

Journal of Ginseng Research

journal homepage: http://www.ginsengres.org

Research Article

# Ameliorative effects of black ginseng on nonalcoholic fatty liver disease in free fatty acid–induced HepG2 cells and high-fat/high-fructose diet-fed mice

Miey Park [1,a], Jeong-Hyun Yoo [2,a], You-Suk Lee [1], Eun-Jung Park [1], Hae-Jeung Lee [1,2,*]

[1] Department of Food and Nutrition, Gachon University, Gyeonggi-do, Republic of Korea
[2] Institute for Aging and Clinical Nutrition Research, Gachon University, Gyeonggi-do, Republic of Korea

ARTICLE INFO

*Article history:*
Received 15 April 2019
Received in Revised form
7 August 2019
Accepted 25 September 2019
Available online 4 October 2019

*Keywords:*
Black ginseng
free fatty acids
high-fat/high-fructose diet
nonalcoholic fatty liver disease

ABSTRACT

*Background:* Black ginseng (BG) is a type of Korean ginseng prepared by steaming and drying raw ginseng to improve the saponin content. This study examined the effects of BG on nonalcoholic fatty liver disease (NAFLD) in HepG2 cells and diet-induced obese mice.
*Methods:* HepG2 cells were treated with free fatty acids to induce lipid accumulation before supplementation with BG. NAFLD-induced mice were fed different doses (0.5%, 1%, and 2%) of BG for 8 weeks.
*Results:* BG significantly reduced lipid accumulation and expression of lipogenic genes, peroxisome proliferator–activated receptor gamma, CCAAT/enhancer-binding protein alpha, sterol regulatory element-binding protein-1c, and fatty acid synthase in HepG2 cells, and the livers of mice fed a 45% high-fat diet with 10% fructose in the drinking water (HFHF diet). BG supplementation caused a significant reduction in levels of aspartate aminotransferase and alanine aminotransferase, while antioxidant enzymes activities were significantly increased in 45% high-fat diet with 10% fructose in the drinking water diet-fed mice. Expression of proliferator-activated receptor alpha and carnitine palmitoyltransferase I were upregulated at the transcription and translation levels in both HepG2 cells and diet-induced obese mice. Furthermore, BG-induced phosphorylation of AMP-activated protein kinase and acetyl CoA carboxylase in both models, suggesting its role in AMP-activated protein kinase activation and the acetyl CoA carboxylase signaling pathway.
*Conclusion:* Our results indicate that BG may be a potential therapeutic agent for the prevention of NAFLD.


## 1. Introduction

Fatty liver is a term used to describe the deposition of more than 5% fat [mainly triglycerides (TGs), phospholipids, and cholesterol ester] in the liver. The major causes of fatty liver include obesity, diabetes, dyslipidemia, alcohol, drugs, hepatitis C, and Wilson's disease [1]. Nonalcoholic fatty liver disease (NAFLD) a type of fatty liver caused by metabolic abnormalities, rather than alcohol or drugs, and may be induced by fructose and other sugars [2]. While NAFLD is not a critical illness, it may progress to various liver diseases such as liver fibrosis, liver cirrhosis, liver failure, and even liver cancer [3]. Therefore, effective prevention and treatment of NAFLD is necessary.

The pathophysiology of NAFLD is closely associated with oxidative stress. Fat deposition in the liver leads to lipid peroxidation and oxidative stress, which promotes various responses such as inflammation and fibrosis. Therefore, antioxidants are proposed candidates for the treatment of NAFLD [4]. To date, there have been no reports on approved therapeutic agents for NAFLD; however, weight loss via diet and exercise is recommended [5]. Drugs that improve insulin resistance or antioxidants (e.g., vitamins E and C) are often used for short-term treatment.

* Corresponding author. Department of Food and Nutrition, Gachon University, Gyeonggi-do 13120, Republic of Korea.
*E-mail addresses:* mieyp@naver.com (M. Park), yjh8252@naver.com (J.-H. Yoo), ysleeyun@gachon.ac.kr (Y.-S. Lee), ejpark@gachon.ac.kr (E.-J. Park), skysea@gachon.ac.kr, skysea1010@gmail.com (H.-J. Lee).
[a] These authors contributed equally to this study.

https://doi.org/10.1016/j.jgr.2019.09.004
p1226-8453 e2093-4947/$ – see front matter 

Many genes play key roles in lipid metabolism. Sterol regulatory element binding protein-1c (SREBP-1c) is a key regulator of cellular lipid homeostasis [6], and peroxisome proliferator-activated receptors (PPARs) are transcription factors involved in lipid homeostasis [7]. In particular, PPARα is expressed in the liver and regulates the expression of genes involved in the mitochondrial β-oxidation pathway and fatty acid metabolism [8]. Hepatic PPARα activity is closely related to the accumulation of liver fat [9]. Carnitine palmitoyltransferase type 1 (CPT-1) transports fatty acids from the cytoplasm to the mitochondria, where they are β-oxidized.

AMP-activated protein kinase (AMPK) is a central regulator of energy homeostasis in tissues and organs [10] and is an important sensor for energy storage, controlling protein synthesis, and other energy-intensive processes [11]. In an energy crisis, activated AMPK shifts cells from an ATP-consuming state to an ATP-producing state [12]. AMPK enhances fatty acid oxidation by reducing the intracellular content of malonyl-CoA, which is an essential precursor for fatty acid biosynthesis and an allosteric inhibitor of CPT-1 [13].

Black ginseng (BG), which is made by steaming and drying Korean ginseng (*Panax ginseng*) several times, contains a large quantities of low-polar ginsenosides, such as Rg3 and Rk1. The functions of BG and its ingredients have been studied and include antioxidant properties and immunomodulation [14–16]. An *in vitro* study showed that hydrogen peroxide–induced reactive oxygen species (ROS) production was attenuated by fermented BG, and the activities of antioxidant enzymes such as catalase (CAT) and superoxide dismutase (SOD) were increased by BG treatment in oxidative stress–induced HepG2 cells [17]. This indicates that BG could be a candidate therapeutic agent for liver diseases [17]. However, the effects of BG on NAFLD remain unclear. Therefore, the present study aimed to determine the effects of BG on NAFLD using *in vitro* and *in vivo* models.

## 2. Materials and methods

### 2.1. BG preparation

Korean ginseng was purchased from Korea Ginseng Agricultural Cooperative Association (Gyeonggi-do, Korea). Powdered BG was prepared by standard production processes and supplied by Do kyung F & S (Gyeonggi-do, Korea). Briefly, washed ginseng was drained and separated into leaves, stems, and roots. The separated materials were placed in a strainer, and the processes of steaming and drying were repeated six to nine times while supplying water at a temperature of 65°C to 95°C. Next, the leaves and roots were ground and used to prepare the experimental diet. The final powdered BG was stored at −20°C until used. Ultra-high-performance liquid chromatography (u-HPLC) analysis was performed according to a previously established method [18].

### 2.2. Cell culture and induction of steatosis

HepG2 cells were purchased from American Type Culture Collection (Manassas, VA) and cultured in Dulbecco's Modified Eagle medium (DMEM) supplemented with 10% fetal bovine serum and 1% antibiotic–antimycotic (Gibco, Grand Island, NY) at 37°C in a humidified atmosphere of 5% $CO_2$. Free fatty acids (FFAs; oleic acid and palmitic acid, 2:1) were dissolved in isopropyl alcohol. HepG2 cells were grown to 80% confiuence then cultured in serum-free medium containing 1% bovine serum albumin (BSA). BG (0, 25, 50, and 100 μg/mL) was added to HepG2 cells induced with 1 mM FFA and incubated for 24 h. Control cells were treated with 1% BSA only.

### 2.3. Cell cytotoxicity detection

Cell Counting Kit-8 (CCK-8) (Dojindo Molecular Technologies, Rockville, MD) was used to determine cytotoxicity [19]. HepG2 cells were seeded at a density of $5 \times 10^4$ cells/well in 96-wells plates and cultured in serum-free DMEM supplemented with 1 mM FFA and 1% BSA and exposed to different concentrations of BG (0, 12.5, 25, 50, 100, and 200 μg/mL) at 37°C for 24 h. After incubation, 10 μL of CCK-8 was added to each well and incubated for 2 h at 37°C. Each experiment was performed in triplicate, and the results were expressed as the percentage of viable cells compared with the control cells. The absorbance was measured at 450 nm using a microplate spectrophotometer system (Epoch Microplate Spectrophotometer; Biotek Inc., Winooski, Vermont).

### 2.4. Oil Red O staining

To detect lipid accumulation, HepG2 cells were fixed with 10% formalin for 10 min then stained with Oil Red O at room temperature for 30 min. The cells were washed three times with deionized water and observed using an optical inverted microscope (Nikon Eclipse, Melville, NY). Lipid quantification in HepG2 cells was performed by eluting the dye with 100% isopropanol and measuring the absorbance at 500 nm. Results were expressed as the percentage of Oil Red O-stained material compared with the control.

### 2.5. Measurement of intracellular TG levels

HepG2 cells were plated in 6-well plates at a density of $1 \times 10^5$ cells/well in serum-free DMEM supplemented with 1 mM FFA and 1% BSA, then allowed to adhere to the wells for 24 h. The cells were treated with different concentrations (0, 25, 50, and 100 μg/mL) of BG and incubated at 37°C for 24 h. TG levels were measured in HepG2 cells using a TG assay kit (Asanpharm, Gyeonggi-do, Korea).

### 2.6. Animals and diets

Four-week-old male imprinting control region (ICR) mice were purchased from Orient Bio Co. Ltd. (Gyeonggi-do, Korea) and housed under a controlled temperature (20-25°C) and humidity (50%–55%) with a 12 h/12 h light–dark cycle. After 7 days of acclimatization, the mice were randomly divided into two groups: normal control group and NAFLD-induced group. The mice had access to food and water ad libitum for 9 weeks and were fed either a normal diet (AIN-93G, D10012G, Research diet, NJ) with normal drinking water or 45% high-fat diet (D12451, Research diet, NJ) with 10% fructose in the drinking water (HFHF). After NAFLD induction, mice were randomized into six groups ($n = 7$ per group) according to body weight: normal diet control (NC), HFHF diet control (HC), HFHF with 1% silymarin (positive control, PC), HFHF with 0.5% (low-dose) BG (LB), HFHF with 1% (medium-dose) BG (MB), and HFHF with 2% (high-dose) BG (HB). The diets were supplemented with BG for 8 weeks. Food intake was monitored once every 2 days, and body weights were measured once a week. The food efficiency ratio (FER) was calculated using the following formula: FER = body weight gain (g)/total food intake (g/day). All animal procedures were approved by Gachon University for the care and use of the laboratory animals (ref. no. GIAUAC -R2017019).

### 2.7. Blood and tissue sample preparation

For blood and tissue collection, mice were fasted overnight, and their final body weights were measured. After 8 weeks, mice were anesthetized using 2%–3% isoflurane (Hana Pharm. Co., Hwasung, Korea) mixed with 70% $N_2O$ and 28.5% $O_2$, using rodent inhalation

**Table 1**
Primer sequence used for quantitative real-time PCR

| | Gene | Forward (5′–3′) | Reverse (5′–3′) |
|---|---|---|---|
| HepG2 | PPARγ | TGCAGGTGATCAAGAAGACG | AGTGCAACTGGAAGAAGGGA |
| | C/EBPα | TGGACAAGAACAGCAACGAGTA | ATTGTCACTGGTCAGCTCCAG |
| | SREBP-1c | GCGCCTTGACAGGTGAAGTC | GCCAGGGAAGTCACTGTCTTG |
| | FAS | CCCCTGATGAAGAAGGATCA | ACTCCACAGGTGGGAACAAG |
| | CPT-1 | CCTCCGTAGCTGACTCGGTA | GGAGTGACCGTGAACTGAAA |
| | PPARα | ACGATTCGACTCAAGCTGGT | GTTGTGTGACATCCCGACAG |
| | β-actin | CTCTTCCAGCCTTCCTTCCT | AGCACTGTGTTGGCGTACAG |
| Mouse liver | PPARγ | CAGGAGAGCAGGGATTTGCA | CCTACGCTCAGCCCTCTTCAT |
| | C/EBPα | TTACAACAGGCCAGGTTTCC | GGCTGGCGACATACAGTACA |
| | SREBP-1c | ATCGCAAACAAGCTGACCTG | AGATCCAGGTTTGAGGTGGG |
| | FAS | TTGCTGGCACTACAGAATGC | AACAGCCTCAGAGCGACAAT |
| | CPT-1 | CTCAGTGGGAGCGACTCTTCA | GGCCTCTGTGGTACACGACAA |
| | PPARα | CAGGAGAGCAGGGATTTGCA | CCTACGCTCAGCCCTCTTCAT |
| | SOD1 | GTGATTGGGATTGCGCAGTA | TGGTTTGAGGGTAGCAGATGAGT |
| | GPX1 | GAAGAACTTGGGCCATTTGG | TCTCGCCTGGCTCCTGTTT |
| | CAT | TGAGAAGCCTAAGAACGCAATTC | CCCTTCGCAGCCATGTG |
| | TNF-α | TGTCCCTTTCACTCACTGGC | CATCTTTTGGGGGAGTGCCT |
| | IL-6 | GGGACTGATGCTGGTGACAA | TCCACGATTTCCCAGAGAACA |
| | NFKB1 | ATTTGAAACACTGGAAGCACGG | CCGCCTTCTGCTTGTAGATAGG |
| | β-actin | CTGTCCCTGTATGCCTCTG | ATGTCACGCACGATTTCC |

PPARγ, peroxisome proliferator-activated receptor gamma; C/EBPα, CCAAT/enhancer-binding protein alpha; SREBP-1c, sterol regulatory element-binding protein1-c; FAS, fatty acid synthase; CPT-1, carnitine palmitoyltransferase-1; PPARα, peroxisome proliferator-activated receptor alpha; SOD, superoxide dismutase; GPX, glutathione peroxidase; CAT, catalase; TNF, tumor necrosis factor; IL, interleukin; NF, nuclear factor

anesthesia apparatus (Surgivet, WI) and a rodent ventilator (Model 687, Harvard Apparatus, Cambridge, UK), and sacrificed. Blood was collected via cardiac puncture and centrifuged (Combi-514R, Hanil Co. Ltd., Seoul, Korea) at 3000 rpm for 15 min at 4°C for serum collection. The abdomens were opened, and fat tissues were removed. Abdominal fat was taken as retroperitoneal and perirenal fat. The retroperitoneal and perirenal fat were removed, and the weight of the abdominal fat was measured. The epididymal fat was weighed separately. The excised fats were rinsed with saline solution to remove blood clots, then the fat depots were weighed, photographed, frozen immediately in liquid nitrogen, and stored at −80°C until used. The liver was removed, rinsed with cold phosphate-buffered saline, and weighed. Small pieces of liver were rapidly excised and frozen immediately using liquid nitrogen for real-time quantitative reverse transcription-polymerase chain reaction and immunoblot analyses. Liver sections for histological evaluation were stored in 10% buffered neutral formalin. The residue was frozen immediately in liquid nitrogen and stored at −80°C.

### 2.8. Serum biochemistry measurements

Levels of serum aspartate aminotransferase (AST) and alanine aminotransferase (ALT) were measured using ALT and AST assay kits (Asanpharm, Hwaseong, Korea). FFA levels were determined using a FFA assay kit (BioAssay Systems, Hayward). High-density lipoprotein (HDL), TG, and total cholesterol (TC) levels were measured using HDL-CHO, TG, and T-CHO kits, respectively, purchased from Asanpharm, Hwaseong, Korea. A colorimetric assay kit (BlueGene Biotech, Shanghai, China) was used to measure serum levels of SOD, glutathione peroxidase (GPx), and CAT. Data were calculated using the formulae described in each kit.

### 2.9. Liver biochemical analysis

Total hepatic TG was extracted according to the method of Folch [20], with some modifications [21]. Approximately 0.1 g of liver tissue was homogenized in 2 mL of chloroform/methanol (2:1, v/v) solution, vortexed, and centrifuged at 3000 rpm for 10 min at room temperature. After centrifugation, the bottom layer was carefully aspirated into a new test tube and evaporated to dryness under a stream of nitrogen. The dried lipid was weighed and redissolved in methanol before lipid analysis. Liver TG content was measured using the TG-S kit (3I1570; Asanpharm, Hwaseong, Korea).

Malondialdehyde (MDA) levels were used as an index of lipid peroxidation [22]. Briefly, 0.1 g of liver tissue was homogenized in 1 mL of KCl (1.15 %) (Sigma–Aldrich, St Louis, MO), followed by the addition of 0.2 mL of sodium dodecyl sulfate (8.1%) (iNtRON Biotechnology, Gyeonggi-do, Korea), 1.5 mL of acetic acid (20%, Daejung Chemical, Suwon, Korea), 1.5 mL of aqueous 2-thiobarbituric acid (0.8%,) (Sigma–Aldrich, Co.), and 0.7 mL of distilled water. Samples were incubated at 95°C for 30 min and cooled on ice. Next, 1 mL of distilled water and 5 mL of *n*-butanol (SAMCHUN, Gyeonggi-do, Korea) were added to the mixture consecutively and vortexed, followed by centrifugation at 4000 rpm for 20 min. MDA levels were calculated in the clear supernatant by measuring the absorbance at 532 nm, and expressed as nmol MDA per weight (g) of liver tissue. A standard curve was calculated using 1,1,3,3-tetraethoxypropane (Sigma–Aldrich).

### 2.10. Histological analysis of liver tissue

Liver tissue was fixed in 10% neural buffered formalin, processed into 3–4 μm sections, and stained with hematoxylin and eosin. The stained sections were observed under an Olympus Provis AX70 microscope (Olympus, Tokyo, Japan), and images were captured using a Nikon DS-Ri2 camera (Nikon, Tokyo, Japan) using NIS-Elements BR 4.50.00 software (Tokyo, Japan) and quantified using ImageJ (NIH).

### 2.11. Real-time RT–PCR for mRNA expression

Total RNA from HepG2 cells and homogenized liver tissue was extracted using an RNA extraction kit (iNtRON Biotechnology, Gyeonggi-do, Korea). RNA (50 ng) was converted to cDNA using the iScript cDNA synthesis kit (BioRad, Hercules, CA). The synthesized cDNA was then used for real-time RT–PCR analysis with SYBR Green Master Mix (TaKaRa Bio, Otsu, Japan) using ABI QuantStudio 3 (Applied Biosystems, Foster City, CA). Details of the primers used in the study are shown in Table 1. Table 1 Gene expression was normalized to β-actin.

**Table 2**
Composition of ginsenosides of black ginseng

| Ginsenosides | Black ginseng (BG) | |
|---|---|---|
| | Leaf (mg/g) | Root (mg/g) |
| Rg1 | 0.00 | 0.12 |
| Re | 0.00 | 0.21 |
| Rf | 0.00 | 0.64 |
| Rh1(S) | 1.77 | 0.84 |
| Rh1(R) | 1.36 | 0.41 |
| Rg2(S) | 3.49 | 1.16 |
| Rg2(R) | 2.43 | 0.64 |
| Rb1 | 0.00 | 3.11 |
| Rc | 0.00 | 1.56 |
| F1 | 0.06 | 0.00 |
| Rb2 | 0.20 | 1.99 |
| Rb3 | 0.08 | 0.30 |
| Rd | 0.93 | 0.98 |
| F2 | 3.83 | 3.56 |
| Rg3(S) | 1.87 | 1.78 |
| Rg3(R) | 1.43 | 1.36 |
| PPT(S) | 0.68 | 0.00 |
| PPT(R) | 1.53 | 0.00 |
| K | 0.13 | 2.34 |
| Rh2(S) | 2.13 | 0.00 |
| Rh2(R) | 1.02 | 0.00 |
| PPD | 0.00 | 0.00 |
| Total ginsenosides[1] | 22.94 | 21.00 |

[1)] Sum of individual ginsenosides content.

### 2.12. Immunoblot analysis

Proteins were extracted from HepG2 cells and liver tissue samples using protein lysis buffer (iNtRON Biotechnology) supplemented with protease and phosphatase inhibitors. Following quantification, 30-μg protein samples were used for separation by 10% sodium dodecyl sulfate polyacrylamide gel electrophoresis. The separated protein bands were transferred to PVDF membranes followed by blocking in 5% skim milk for 1 h at room temperature. After washing, the membranes were immunoblotted using primary antibodies against PPARγ, CCAAT/enhancer-binding protein alpha (C/EBPα), SREBP-1c, fatty acid synthase (FAS), PPARα, CPT-1, acetyl CoA carboxylase (ACC), p-ACC, AMPK, and p-AMPK for 2 h at room temperature. After three washes, the membranes were incubated with anti-mouse or anti-rabbit horseradish peroxidase-conjugated secondary antibodies in 5% skim milk for 1 h at room temperature. Reactive band signals were detected using an ECL Western blot detection kit (Amersham Pharmacia, Little Chalfont, Bucks, UK) and visualized using image quant LAS 500 (GE Healthcare Bio-Sciences AB, Sweden).

### 2.13. Data analyses

Three separate experiments were each performed in triplicate. Statistical analyses were performed using GraphPad prism 5.03 (GraphPad Software, San Diego, CA) with one-way analysis of variance and Tukey's post hoc tests. Analysis of the animal experiments was conducted using SPSS software, version 23, (SPSS Inc., Chicago, IL, USA). Experimental data were expressed as mean ± standard deviation (n = 7 per group). One-way analysis of variance with Duncan's multiple range test assessed differences between mean values for individual groups. Differences with values of $p < 0.05$ were considered statistically significant.

## 3. Results

### 3.1. Quantification of ginsenosides in BG

HPLC analysis of BG revealed that it contained various ginsenosides (Table 2). In total, 22 different types of ginsenosides with varied composition were quantified by u-HPLC in the leaves and roots. The most abundant component in the leaves was F2 (3.83 mg/g), followed by Rg2(S) (3.49 mg/g), Rg2(R) (2.43 mg/g), Rh2(S) (2.13 mg/g), and Rg3(S) (1.87 mg/g). The predominant component

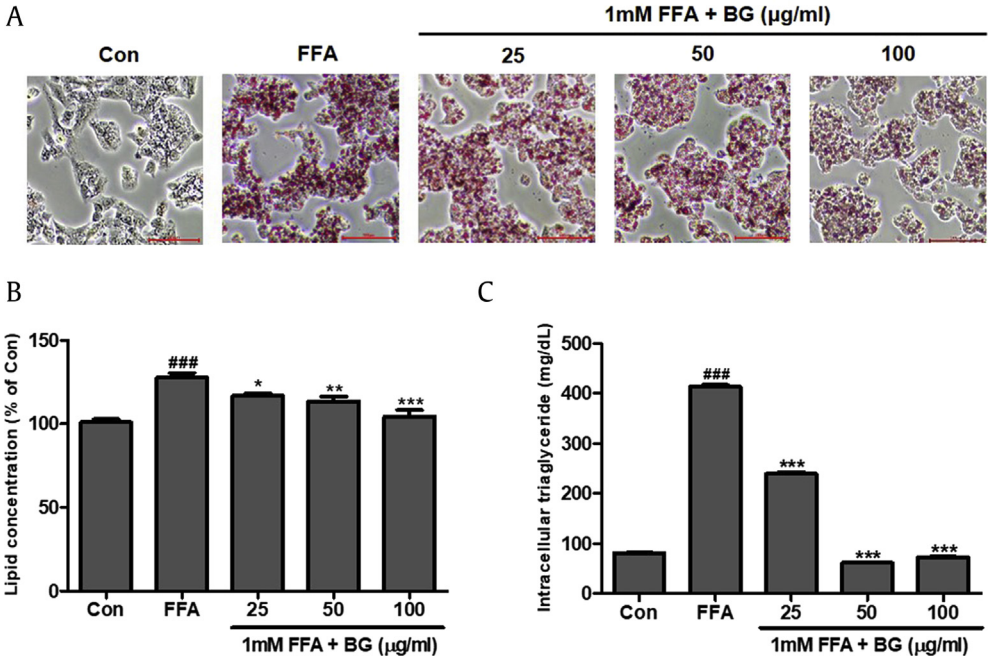


**Fig. 1. Effect of black ginseng (BG) on 1 mM FFA-induced lipid accumulation in HepG2 cells.** (A) Oil Red O staining images of HepG2 cells treated with 1 mM free fatty acids (FFAs) and various concentration of BG for 24 h. Control cells (Con) were incubated with 1% fat-free BSA. Lipid droplets of HepG2 cells were dyed red (magnification 200×). (B) Lipid accumulation of Oil Red O contents was quantified by spectrophotometric analysis at 500 nm. (C) Quantification of intracellular triglycerides in HepG2 cells. The BG (0, 25, 50, and 100 μg/ml) was added to the 1mM FFA-induced HepG2 cells and incubated for 24h. Data represent means ± SD. $^{###}p < 0.001$ vs. Con; $^{*}p < 0.05$, $^{**}p < 0.01$, $^{***}p < 0.001$ vs. FFA.

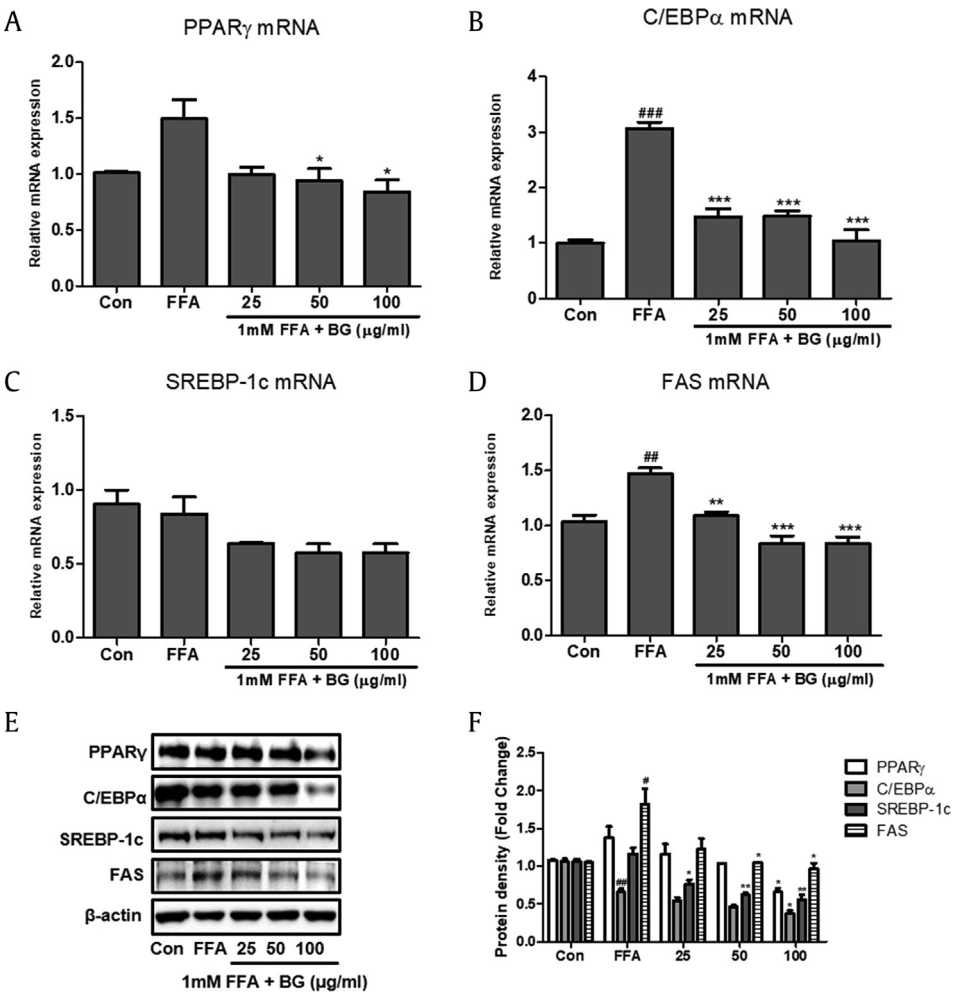


**Fig. 2. Effect of BG on the expression of lipogenic markers in HepG2 cells.** Quantitative real-time PCR analysis of PPARγ (A), C/EBPα (B), SREBP-1c (C), and FAS (D) were normalized by β-actin as an internal control. (E) Western blot analysis of PPARγ, C/EBPα, SREBP-1c, and FAS. (F) Relative protein levels of PPARγ, C/EBPα, SREBP-1c, and FAS. Equal loading of protein was verified by β-actin. The BG (0, 25, 50, and 100 μg/ml) was added to the 1mM FFA-induced HepG2 cells and incubated for 24h. Results of three independent experiments are represented the means ± SD. $^{\#}p < 0.5$, $^{\#\#}p < 0.01$, $^{\#\#\#}p < 0.001$ vs. Con; $^{*}p < 0.05$, $^{**}p < 0.01$, $^{***}p < 0.001$ vs. FFA. PPARγ, peroxisome proliferator-activated receptor gamma; C/EBPα, CCAAT/enhancer-binding protein alpha; SREBP-1c, sterol regulatory element-binding protein1-c; FAS, fatty acid synthase; FFA, free fatty acid; BG, black ginseng.

in the roots was also F2 (3.56 mg/g), followed by Rb1 (3.11 mg/g, which was not detected in leaves), K (2.34 mg/g), Rb2 (1.99 mg/g), and Rg3(S) (1.78 mg/g). The total ginsenoside content was 22.94 in the leaves and 21.00 mg/g and in the roots.

### 3.2. Effects of BG on cell viability and FFA-induced steatosis

HepG2 cells were treated with different concentrations of BG plus 1 mM FFA for 24 h to induce hepatic steatosis. Control cells (Con) were treated with 1% BSA only. BG treatment up to 200 μg/mL with 1 mM FFA for 24 h did not decrease cell viability (Suppl. Fig. 1). Intracellular lipid accumulation was visually observed by Oil Red O staining (Fig. 1A). Lipid droplets were significantly increased in HepG2 cells with FFA-induced steatosis compared with control cells. Furthermore, BG treatment significantly attenuated lipid and intracellular TG accumulation in HepG2 cells (Fig. 1B and C).

### 3.3. Effects of BG on lipogenesis in FFA-induced steatosis

To investigate whether BG attenuated FFA-induced steatosis, we measured expression of the lipogenic factors PPARγ, C/EBPα, SREBP-1c, and FAS using real-time RT–PCR and immunoblot analysis. The relative mRNA expression of PPARγ, C/EBPα, and FAS was significantly increased in cells treated with 1 mM FFA compared with control cells (Fig. 2). SREBP-1c expression was downregulated in response to BG treatment compared with steatosis-induced HepG2 cells. However, BG treatment significantly downregulated the relative mRNA expression of PPARγ, C/EBPα, and FAS. In addition, a significant decrease in protein levels was also observed after BG treatment compared with HepG2 cells treated with 1 mM FFA.

### 3.4. Effects of BG on PPARα, CPT-1, and phosphorylation of AMPK and ACC in FFA-induced steatosis

Expression of PPARα and CPT-1 was increased in a dose-dependent manner in response to BG treatment in FFA-induced HepG2 cells at both the transcriptional and translational level (Fig. 3A–D). FFA-induced steatosis abated phosphorylation levels of AMPK and ACC in HepG2 cells. However, 24-h BG treatment led to a significant increase in phosphorylation of AMPK and ACC (Fig. 3E and F).

### 3.5. Effects of BG on body weight, organ weight, and food intake in NAFLD-induced mice

HFHF-fed animals were categorized according to initial body weight (between 49.53 and 51.96 g) (Fig. 4A). After eight weeks on

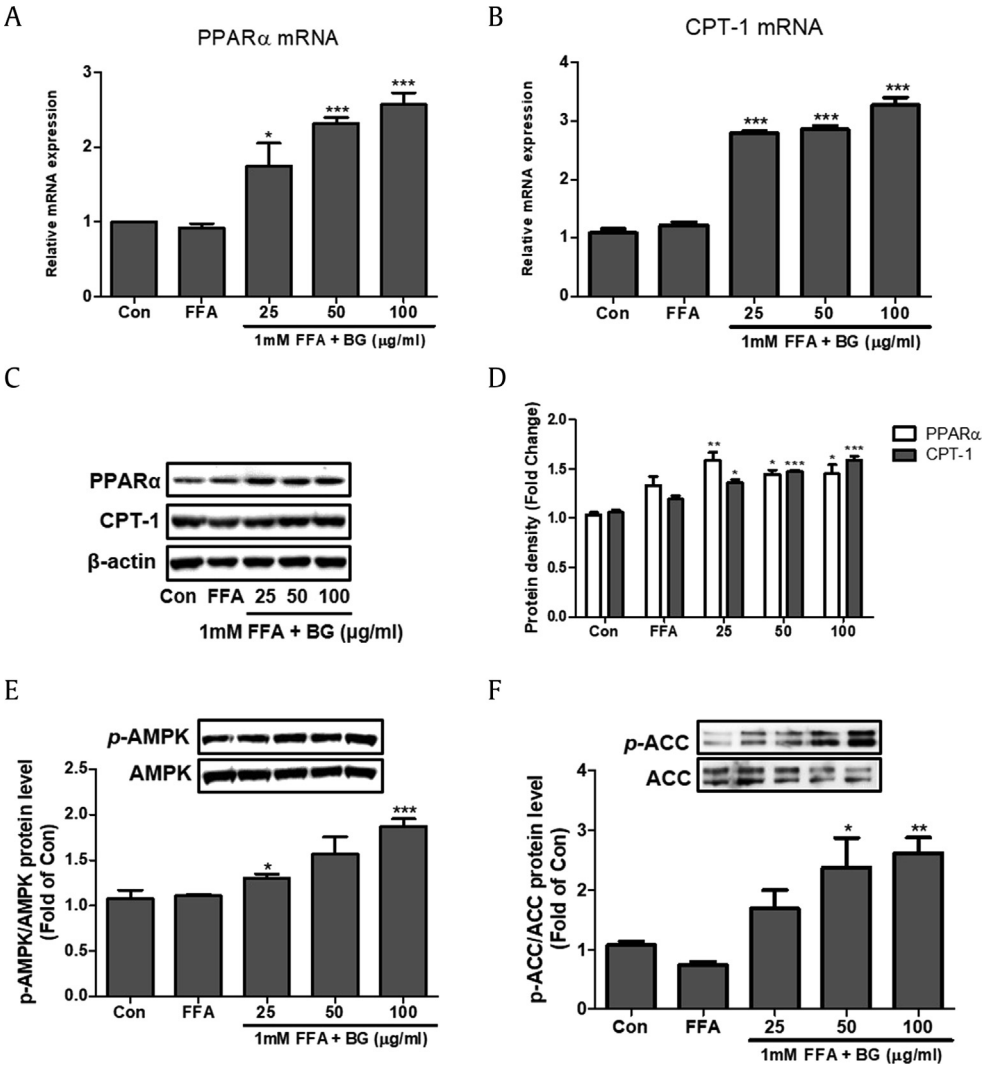


**Fig. 3. Effect of BG on fatty acid oxidation and AMPK and ACC signaling in HepG2 cells treated with 1 mM FFA.** The mRNA expression of PPARα (A) and CPT-1 (B) were quantified by real-time PCR and normalized by β-actin. (C) PPARα and CPT-1 protein levels by immunoblot analysis. (D) Quantification of the protein levels of PPARα and CPT-1. Equal loading of protein was verified by β-actin. (E) Western blot analysis of AMP-activated protein kinase (AMPK). (F) Western blot analysis of acetyl-CoA carboxylase (ACC). AMPK and ACC were used as a protein loading control of phosphorylated AMPK (p-AMPK) and phosphorylated ACC (p-ACC), respectively. The BG (0, 25, 50, and 100 μg/ml) was added to the 1mM FFA-induced HepG2 cells and incubated for 24h. Results of three independent experiments are expressed as the mean ± SD. $^{*}p < 0.05$, $^{**}p < 0.01$, $^{***}p < 0.001$ vs. FFA. FFA, free fatty acid; BG, black ginseng; CPT-1, carnitine palmitoyltransferase-1; PPARα, Peroxisome proliferator-activated receptor alpha.

their assigned diets, the terminal body weights of the mice were not significantly different among the HFHF diet-induced NAFLD groups.

The liver, abdominal, and epididymal adipose tissue weights of the mice are presented in Table 3. After comparing relative organ weights, the liver weights were not significantly different among the HFHF diet-induced NAFLD groups. However, the abdominal and epididymal adipose tissue weights of the HC group were significantly increased compared with the NC group. No significant difference between the experimental groups was observed; however, in the HB group, the weight of abdominal adipose tissue was significantly decreased (Table 3).

Suppl. Table 1 shows the food intake and FER. Dietary intake during the eight weeks increased in the following order: HC < NC < LB < HB < MB < PC groups ($p < 0.05$). The HC group showed the lowest food intake, but highest FER. In contrast, higher food intake and lower FER ratios were observed in BG groups compared with the HC group.

### 3.6. Effects of BG on serum biochemical parameters

AST and ALT enzyme activities were measured to investigate the effect of BG in steatosis-induced animal models. BG treatment significantly decreased the elevated AST (Fig. 4B) and ALT (Fig. 4C) levels seen in the HC group. FFA and HDL-cholesterol levels were measured to examine the effects of BG on serum lipid profiles. As shown in Fig. 5, serum FFA levels were significantly increased in the HC group compared with the NC group. However, FFA levels were significantly reduced after BG treatment (Fig. 5A). HDL-cholesterol levels were increased in the HB group compared with those of the HC group. There was no significant difference in the LB and MB groups, but BG intake led to a tendency towards an increase in HDL-cholesterol levels (Fig. 5B and Suppl. Table 1). No significant differences were observed in serum TG levels among the groups (Fig. 5C). TC levels were significantly higher in the HC group compared with those of the NC group. In contrast, the BG diet led to significantly decreased TC levels compared with the HC group (Fig. 5D).

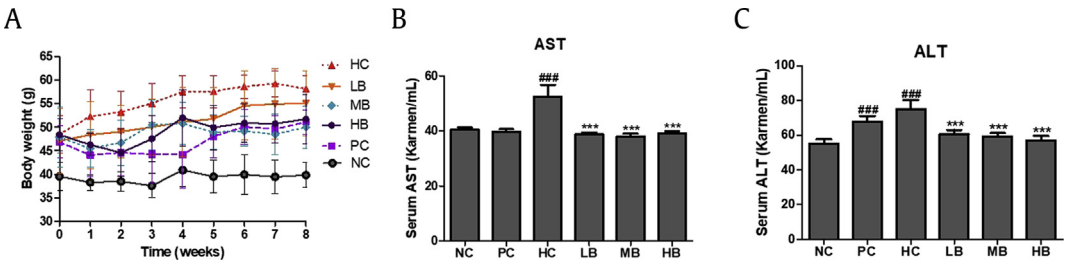


**Fig. 4. Effect of BG on the body weight and serum AST and ALT in high fat diet with 10% fructose (HFHF) fed mice.** (A) Body weight during experimental stage. (B) Serum AST. (C) Serum ALT. AST, aspartate transaminase; ALT, alanine transaminase; NC, Normal control; HC, 45% high fat diet with 10% fructose in the drinking water (HFHF) control; PC, positive control (HFHF + 1% silymarin); LB, low-dose BG (HFHF + 0.5% BG); MB, middle-dose BG (HFHF + 1% BG); HB, high-dose BG (HFHF + 2% BG); BG, black ginseng. Values are expressed as mean ± SD. $^{###}p < 0.001$ vs. Con; $^{***}p < 0.001$ vs. FFA.

To further evaluate the antioxidant effect of BG, serum enzyme activities of SOD, GPx, and CAT were measured by colorimetric assay. The results showed lower activities of SOD, GPx, and CAT in the HC group. However, BG treatment significantly increased levels of SOD, GPx, and CAT compared with the HC group (Fig. 5E–G).

### 3.7. Effects of BG on hepatic steatosis in NAFLD-induced mice

Fig. 6A shows the histological analysis of the liver in the six groups. In the HC group, the liver showed numerous and widespread lipid droplets. However, the HFHF diet induced pathological changes (increased size of fat droplets), while there was a noticeable decrease in lipid accumulation in the BG groups. To examine the effects of BG on hepatic biochemical parameters, hepatic TG and MDA levels were measured in the steatosis-induced animal model. As shown in Fig. 6B and C, the HFHF diet led to prominent lipid accumulation in the livers of the experimental mice. Hepatic TG levels were significantly higher in the HC group compared with the NC group. However, BG supplementation inhibited HFHF diet-induced hepatic TG accumulation compared with the HC group (Fig. 6B). Similarly, hepatic MDA levels were significantly elevated in the HC group compared with those of the NC group (Fig. 6C), while a significant reduction was observed in the BG-treated groups. Macrovesicular fatty changes were calculated by measuring the area of the fat droplets. Macrovesicular steatosis levels were significantly higher in the HC group compared with the other group (Fig. 6D).

### 3.8. Effects of BG on hepatic lipid gene expression in NAFLD-induced mice

To investigate the molecular mechanisms of BG on TG accumulation in the liver, regulators of lipogenesis were examined by real-time RT–PCR and immunoblot analysis. There was a significant upregulation of mRNA expression of PPARγ, C/EBPα, SREBP-1c, and FAS in the livers of mice in the HC group compared with the NC group. In the BG-supplemented groups, mRNA expression of PPARγ, C/EBPα, SREBP-1c, and FAS was significantly decreased compared with that in the HC group (Fig. 7A–D). In line with this, immunoblot analysis showed a dose-dependent downregulation of protein levels of PPARγ, C/EBPα, SREBP-1c, and FAS in the BG-supplemented groups (Fig. 7E and F).

### 3.9. Effects of BG on lipid metabolism and phosphorylation of AMPK and ACC in NAFLD-induced mice

Expression of genes involved in fatty acid oxidation, such as CPT-1 and PPARα, were evaluated. Real-time RT–PCR showed significant upregulation of CPT-1 and PPARα mRNA expression in the BG-supplemented groups (LB, MB, and HB) compared with the HC group (Fig. 8A and B). Consistent with this, immunoblot analysis showed elevated protein levels of CPT-1 and PPARα in response to BG treatment (Fig. 8C and D).

We assessed the expression of antioxidant enzymes (Suppl. Fig. 2). The mRNA expression of antioxidant enzymes in NAFLD-induced mice revealed significantly decreased expression of SOD1, GPX, and CAT enzymes in the HC group compared with the NC group, but significantly increased expression levels in the BG-treated groups. Significantly increased expression levels were reported in the BG-supplemented groups (LB, MB, and HB).

Immunoblot analysis was performed to examine the effect of the HFHF diet on the activation of AMPK and ACC in the presence of BG. The results showed decreased levels of phosphorylation of AMPK and ACC in the HC group, while BG treatment resulted in significant dose-dependent activation of AMPK and ACC via phosphorylation (Fig. 8E and F).

**Table 3**
Body weight and relative organ weight of each group

| Groups | Body weights | | | Relative organ weight (%) | | |
|---|---|---|---|---|---|---|
| | Body weight prior to drug treatment (g) [A] | Terminal body weight (g) [B] | Body weight gains [B-A] | Liver | Abdominal adipose tissue | Epididymal adipose tissue |
| NC | $40.54 \pm 4.31^{b}$ | $40.31 \pm 2.36^{b}$ | $-0.23 \pm 3.48^{b}$ | $4.06 \pm 0.85^{ns}$ | $0.48 \pm 0.41^{b}$ | $2.55 \pm 1.44^{b}$ |
| PC | $51.16 \pm 8.07^{a}$ | $55.10 \pm 7.16^{a}$ | $3.94 \pm 1.82^{ab}$ | $4.18 \pm 0.57$ | $1.20 \pm 0.50^{a}$ | $4.73 \pm 1.14^{a}$ |
| HC | $51.43 \pm 6.06^{a}$ | $55.29 \pm 6.15^{a}$ | $3.86 \pm 3.27^{ab}$ | $4.41 \pm 0.97$ | $1.41 \pm 0.41^{a}$ | $4.52 \pm 1.19^{a}$ |
| LB | $49.53 \pm 7.51^{a}$ | $57.61 \pm 7.15^{a}$ | $8.09 \pm 4.75^{a}$ | $4.45 \pm 0.41$ | $1.38 \pm 0.66^{a}$ | $4.25 \pm 0.99^{a}$ |
| MB | $49.53 \pm 7.02^{a}$ | $53.60 \pm 7.19^{a}$ | $4.07 \pm 6.05^{ab}$ | $4.57 \pm 0.64$ | $1.26 \pm 0.96^{a}$ | $4.07 \pm 0.88^{a}$ |
| HB | $51.96 \pm 5.44^{a}$ | $55.19 \pm 7.05^{a}$ | $3.23 \pm 4.46^{ab}$ | $4.86 \pm 0.59$ | $1.09 \pm 0.48^{ab}$ | $4.22 \pm 1.22^{a}$ |

NC, normal control; HC, 45% high fat diet with 10% fructose in the drinking water (HFHF) control; PC, positive control (HFHF + 1% silymarin); LB, low-dose black ginseng (HFHF + 0.5% black ginseng); MB, middle-dose black ginseng (HFHF + 1% black ginseng); HB, high-dose black ginseng (HFHF + 2% black ginseng). Body weight prior to drug treatment was randomized body weight after 9 weeks of induction period of NAFLD.. Values are expressed as mean ± SD. Different letters (a > b) within a column indicate significant differences ($p < 0.05$) determined by Duncan's multiple range test. $^{ns}$, not significant

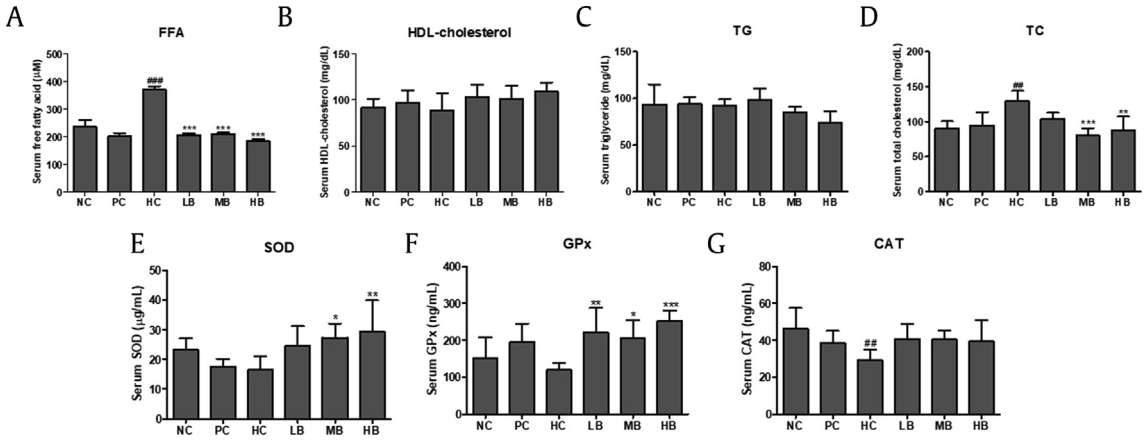


**Fig. 5. Effect of BG on the serum lipid profiles of NAFLD-induced mice.** (A) FFA; (B) HDL; (C) TG; (D) TC. (E) SOD. (F) GPx. (G) CAT. FFA, free fatty acid; HDL, high density lipoprotein cholesterol; TG, triglyceride; TC, total cholesterol; SOD, superoxide dismutase; GPx, glutathione peroxidase; CAT, catalase; NC, normal control; HC, 45% high fat diet with 10% fructose in the drinking water (HFHF) control; PC, positive control (HFHF + 1% silymarin); LB, low-dose BG (HFHF + 0.5% BG); MB, middle-dose BG (HFHF + 1% BG); HB, high-dose BG (HFHF + 2% BG); NAFLD, nonalcoholic fatty liver disease; BG, black ginseng. The results from three independent experiments are expressed as the mean ± SD. $^{\#\#}p < 0.01$, $^{\#\#\#}p < 0.001$ vs. NC; $^{*}p < 0.05$, $^{**}p < 0.01$, $^{***}p < 0.001$ vs. HC.

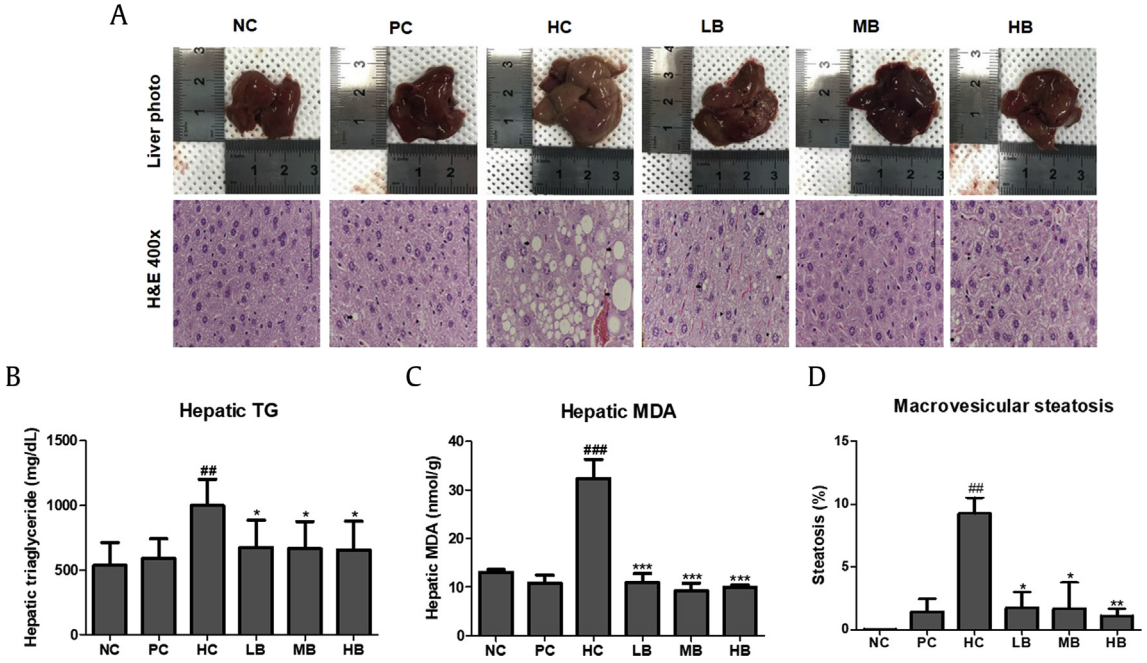


**Fig. 6. Effect of BG treatment on hepatic steatosis in normal or NAFLD-induced mice.** (A) Liver tissue histology (400 ×). (B) The accumulation of liver TG. (C) Hepatic MDA levels. (D) Macrovesicular fatty changes in hepatocytes. H&E, hematoxylin and eosin; TG, triglyceride; MDA, malondialdehyde; NC, normal control; HC, 45% high fat diet with 10% fructose in the drinking water (HFHF) control; PC, positive control (HFHF + 1% silymarin); LB, low-dose BG (HFHF + 0.5% BG); MB, middle-dose BG (HFHF + 1% BG); HB, high-dose BG (HFHF + 2% BG); NAFLD, nonalcoholic fatty liver disease; BG, black ginseng. The results from three independent experiments are expressed as the mean ± SD. $^{\#\#}p < 0.01$, $^{\#\#\#}p < 0.001$ vs. NC; $^{*}p < 0.05$, $^{***}p < 0.001$ vs. HC.

## 4. Discussion

BG differs from white or red ginseng in its appearance and ginsenoside composition due to the steaming and drying process. The steaming process used to produce BG enhances the biological activity of the raw material and converts major saponins [16], polar molecules such as Rg1, Re, Rc, and Rd, to low-polar molecules such as 20(S)/20(R)-Rg2, 20(S)/20(R)-Rg3, Rh1, and Rk1] [23]. The beneficial effects of low-polar ginsenosides have been steadily reported and include antioxidant, neuroprotective, and anticancer functions [24,25]. Our results demonstrated that the BG used in the study comprised low-polar ginsenosides, with the highest content of F2 in both the leaves and roots. Ginsenoside F2 has been reported to be synthesized from Rb1, Rb2, and Rd via hydrolysis [26], and finally converted to compound K, which is a major absorption type of ginsenoside [27]. The roots used in the present study contained large amounts of compound K. Biological studies have shown that ginsenoside K exhibits multiple pharmacological properties [27]. Similarly, our results indicated that the BG used in this study had the potential to improve NAFLD, as shown using *in vitro* and *in vivo* models.

NAFLD is one of the leading causes of chronic liver disease. Obesity caused by excessive nutrition is a major risk factor for NAFLD. Recent *in vivo* studies have shown that high-fat/high-

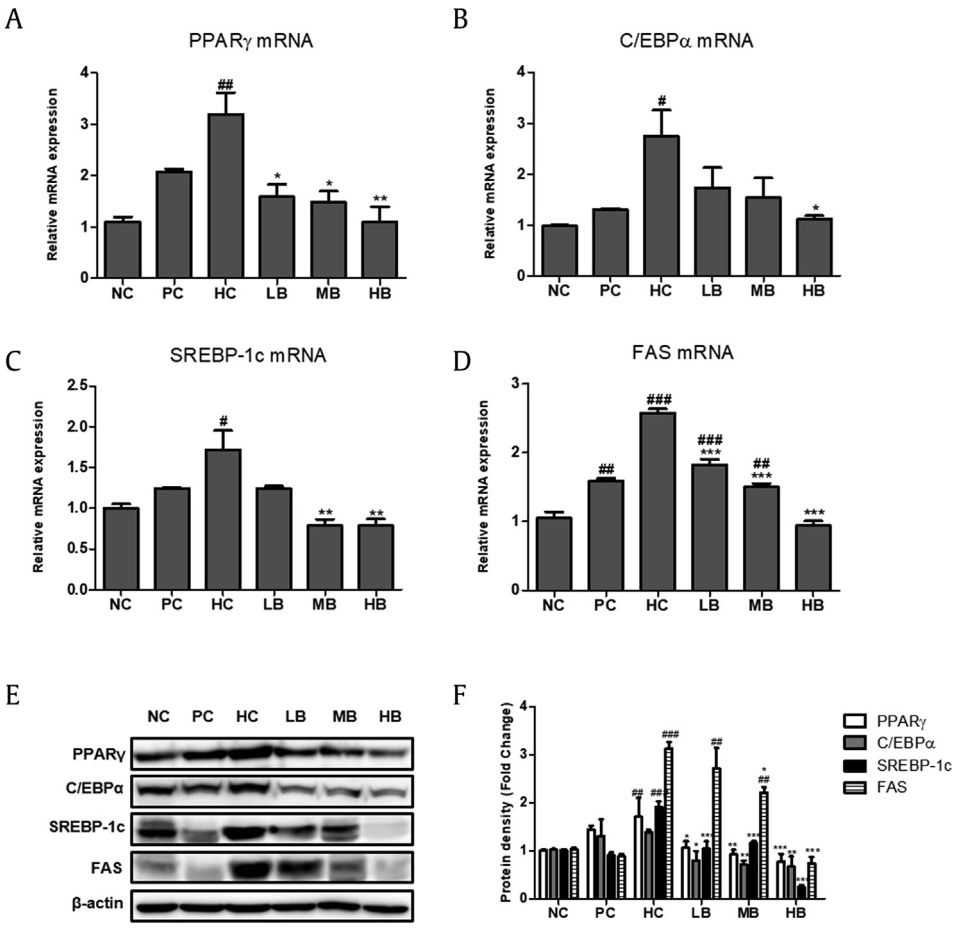


**Fig. 7. Effect of BG on the expression of lipogenic markers in NAFLD-induced mice.** Quantitative real-time PCR analysis of PPARγ (A), C/EBPα (B), SREBP-1c (C), and FAS (D) were normalized by β-actin. (E) Western blot analysis of PPARγ, C/EBPα, SREBP-1c, and FAS. (F) Relative protein levels of PPARγ, C/EBPα, SREBP-1c, and FAS. Equal loading of protein was verified by β-actin. NC, normal control; HC, 45% high fat diet with 10% fructose in the drinking water (HFHF) control; PC, positive control (HFHF + 1% silymarin); LB, low-dose BG (HFHF + 0.5% BG); MB, middle-dose BG (HFHF + 1% BG); HB, high-dose BG (HFHF + 2% BG); NAFLD, nonalcoholic fatty liver disease; BG, black ginseng; PPARγ, peroxisome proliferator-activated receptor gamma; C/EBPα, CCAAT/enhancer-binding protein alpha; SREBP-1c, sterol regulatory element-binding protein1-c; FAS, fatty acid synthase. The results from three independent experiments are expressed as the mean ± SD. $^{\#\#}p < 0.01$, $^{\#\#\#}p < 0.001$ vs. NC; $^{*}p < 0.05$, $^{**}p < 0.01$, $^{***}p < 0.001$ vs. HC.

fructose diets increase liver fat accumulation [28,29]. In the present study, a HFHF diet (45% high fat diet with 10% fructose in the drinking water) was used to induce NAFLD in an animal model for 9 weeks, and the hepatic histological appearance confirmed that the HFHF diet induced changes in hepatic lipid accumulation. Therefore, we successfully established a HFHF diet-induced fatty liver animal model to evaluate the effects of BG on NAFLD.

Serum ALT and AST levels are closely related to hepatocellular health state, and damage to the liver, whether acute or chronic, leads to elevated serum concentrations of these enzymes. In the present study, the highest concentrations of ALT and AST were reported in the HC group, while BG treatment in the different groups led to a significant reduction of both these enzymes. Our results are in accordance with a previous *in vivo* study that showed that BG attenuated elevated ALT and AST levels in an acetaminophen-induced liver damage mouse model [30]. The results show strong evidence *in vivo* for the protective effect in liver of BG, especially in NAFLD.

Many studies have shown that serum FFAs play a pivotal role in the development of NAFLD, and act as strong oxidants [31]. The levels of FFAs entering the liver also increase proportionately, and the FFAs that enter the liver are converted to TG and accumulate in the liver. Our results showed that not only serum FFA was increased, but that hepatic TG was also increased in both *in vivo* and *in vitro* models. These changes in FFA-treated HepG2 cells and HFHF diet-fed mice were decreased in the presence of BG. These observations indicated that BG affected the accumulation of TG and serum FFA levels in HepG2 cells and mouse liver. While serum HDL-cholesterol levels were increased, serum TC levels were decreased by BG treatment. A previous study reported that BG extracts play an important role in regulating the effects of hypercholesterolemia via modulation of markers of cholesterol metabolism such as acetyl-CoA acetyltransferase 2, SREBP2, and 3-hydroxy-3-methyl-glutaryl-coenzyme A reductase [32]. Furthermore, studies have reported that dietary saponins increase fecal excretion of bile acids and may lower plasma cholesterol concentrations in hypercholesterolemic patients [33]. Dietary BG supplementation has been reported to increase fecal weight and fecal lipid excretion [34]. These results suggest that consumption of BG can positively affect lipid metabolism.

The pathophysiology of NAFLD is associated with oxidative stress. Imbalance between ROS and antioxidant capacity leads to lipid peroxidation and ultimately cellular damage, leading to fibrogenesis [35]. Cellular antioxidant defenses against such oxidative stress involve antioxidant enzymes such as SOD, GPx, and CAT. We showed that serum enzyme activities and hepatic mRNA expression levels of SOD, GPx, and CAT were significantly decreased

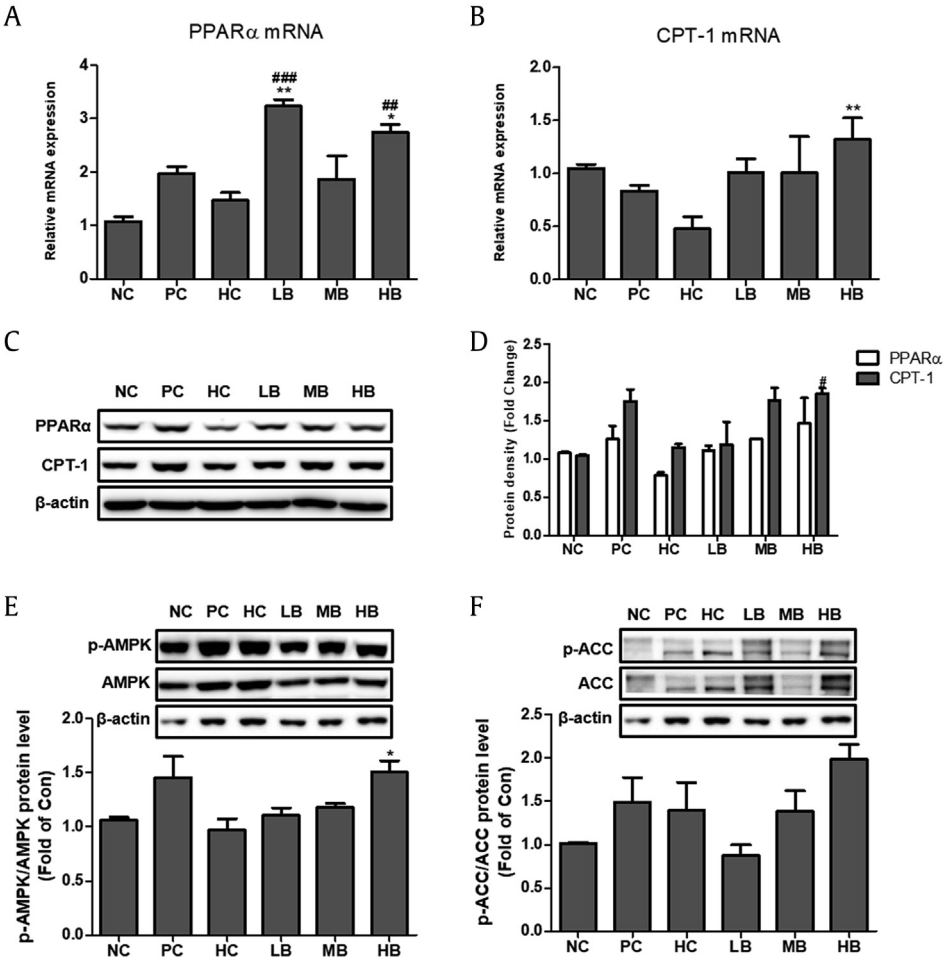


**Fig. 8. Effect of BG on fatty acid oxidation and AMPK and ACC signaling in NAFLD-induced mice.** The mRNA expression of PPARα (A) and CPT-1 (B) were quantified by real-time PCR and normalized by β-actin as an internal control. (C) PPARα and CPT-1 protein levels by immunoblot analysis. (D) Quantification of the protein levels of PPARα and CPT-1. (E) Western blot analysis of AMP-activated protein kinase (AMPK) (F) Western blot analysis of acetyl-CoA carboxylase (ACC). AMPK and ACC were used as a protein loading control of phosphorylated AMPK (p-AMPK) and phosphorylated ACC (p-ACC), respectively. NC, normal control; HC, 45% high fat diet with 10% fructose in the drinking water (HFHF) control; PC, positive control (HFHF + 1% silymarin); LB, low-dose BG (HFHF + 0.5% BG); MB, middle-dose BG (HFHF + 1% BG); HB, high-dose BG (HFHF + 2% BG); BG, black ginseng; NAFLD, nonalcoholic fatty liver disease. The results from three independent experiments are expressed as the mean ± SD. $^{\#\#}p < 0.01$, $^{\#\#\#}p < 0.001$ vs. NC; $^{*}p < 0.05$, $^{**}p < 0.01$ vs. HC.

in the HC group, while serum enzyme and hepatic mRNA expression levels of each antioxidant enzymes were significantly increased in the BG-supplemented groups (LB, MB, and HB). Taken together, it can be inferred from these results that BG protects the liver from damage by regulating the antioxidant enzyme defense system. Ginsenosides possess strong antioxidant activity via activation of nuclear factor erythroid 2-related factor (Nrf2)—antioxidant responsive element (ARE)-mediated pathway [36]. Nrf2 is a transcription factor that plays a key role in activation of the antioxidant defense system. Under conditions of oxidative stress, Nrf2 is synthesized de novo in the cytoplasm then translocates to the nucleus where it activates antioxidant target genes, such as SOD, GPx, CAT, and heme oxygenase-1, by binding to regulatory AREs. In the present study, expression of antioxidant enzymes was upregulated by BG treatment. Further studies are required to confirm the involvement of the Nrf2—ARE pathway.

NAFLD is characterized by ectopic accumulation of fat in the liver, which increases the potential risk of ROS production and depletion of antioxidants. Excessive ROS production promotes lipid peroxidation, which subsequently leads to the formation of other reactive metabolites in the liver, such as trans-4-hydroxy-2-nonenal and MDA [37]. The present study showed a significant difference in hepatic TG and MDA levels between the HC and NC groups. A significant reduction was observed in TG and MDA levels in the BG-treated groups compared with the HC group. We found that BG played an important hepatoprotective role via elimination of hepatic TG accumulation and lipid peroxidation, upregulation of the antioxidant activity and expression, and improved lipid profiles (in particular, regulation of FFA levels).

Furthermore, expression of lipogenesis-related genes, PPARγ, C/EBPα, SREBP-1c, and FAS, were elevated in HepG2 cells treated with 1 mM FFA and the livers of HFHF diet-fed mice. BG treatment decreased the expression of lipogenesis markers. In addition, phosphorylation of AMPK and ACC was significantly increased by supplementation with BG. These results suggested that BG may act to reduce hepatic steatosis by increasing AMPK phosphorylation. Reduced AMPK activity is associated with NAFLD-related conditions such as inflammation, obesity, and diabetes. Therefore, increasing AMPK activity is considered a viable treatment strategy to improve NAFLD [38]. AMPK has a direct effect on lipid metabolism by inhibiting fat accumulation via modulation of several downstream signal components, such as ACC, which is a primary target enzyme [39]. In addition, AMPK can mediate the expression of factors related to fatty acid oxidation, such as PPARα and CPT-1 [40]. PPARα eliminates the major source of lipid accumulation in NAFLD, including dietary fatty acids and FFA released from

adipocytes [41]. CPT-1 is the key regulatory enzyme of long-chain fatty acid β-oxidation in the outer membrane of mitochondria and attenuates fatty acid–induced insulin resistance and inflammation [42,43]. Our results showed that BG suppressed TG synthesis and reduced cellular lipid accumulation by increasing phosphorylation of AMPK and ACC, which are important regulators of fatty acid oxidation and hepatocellular lipid metabolism. These results demonstrate that BG may have pharmacological effects on NAFLD by targeting the AMPK signaling pathway.

The present study showed the effects of BG on NAFLD in FFA-induced HepG2 cells and HFHFD diet-fed ICR mice. BG decreased serum TG and TC levels and downregulated expression of lipogenesis factors, including PPARγ, C/EBPα, SREBP-1c, and FAS, at the transcriptional and translational levels, while expression of fatty acid oxidation–related genes was significantly upregulated. Furthermore, BG induced phosphorylation of AMPK and ACC *in vitro* and *in vivo*. These factors led to a decrease in FFA uptake and TG synthesis. Our findings suggest that BG could prevent hepatic steatosis and ameliorate fatty liver disease by suppressing lipogenesis. Taken together, our findings highlight the use of BG as a potential therapeutic agent or functional food material for NAFLD treatment.

## Conflicts of interest

All contributing authors declare no conflicts of interest.

## Acknowledgments

This work was supported by a grant “Food Functionality Evaluation program” under the Ministry of Agriculture, Food and Rural Affairs and partly Korea Food Research Institute awarded in 2017.

## Appendix A. Supplementary data

Supplementary data to this article can be found online at https://doi.org/10.1016/j.jgr.2019.09.004.

## References

[1] Brunt EM. Nonalcoholic fatty liver disease: what the pathologist can tell the clinician. Digestive Diseases (Basel, Switzerland) 2012;30(1):61–8.
[2] Jensen T, Abdelmalek MF, Sullivan S, Nadeau KJ, Green M, Roncal C, et al. Fructose and sugar: a major mediator of non-alcoholic fatty liver disease. Journal of Hepatology 2018;68(5):1063–75.
[3] Adams LA, Lymp JF, St Sauver J, Sanderson SO, Lindor KD, Feldstein A, Feldstein A, Angulo P. The natural history of nonalcoholic fatty liver disease: a population-based cohort study. Gastroenterology 2005;129(1):113–21.
[4] Salomone F, Godos J, Zelber-Sagi S. Natural antioxidants for non-alcoholic fatty liver disease: molecular targets and clinical perspectives. Liver International : Official Journal of the International Association for the Study of the Liver 2016;36(1):5–20.
[5] Romero-Gomez M, Zelber-Sagi S, Trenell M. Treatment of NAFLD with diet, physical activity and exercise. Journal of Hepatology 2017;67(4):829–46.
[6] Kamei Y, Miura S, Suganami T, Akaike F, Kanai S, Sugita S, Katsumata A, Aburatani H, Unterman TG, Ezaki O, Ogawa Y. Regulation of SREBP1c gene expression in skeletal muscle: role of retinoid X receptor/liver X receptor and forkhead-O1 transcription factor. Endocrinology 2008;149(5):2293–305.
[7] Krey G, Braissant O, L'Horset F, Kalkhoven E, Perroud M, Parker MG, Wahli W. Fatty acids, eicosanoids, and hypolipidemic agents identified as ligands of peroxisome proliferator-activated receptors by coactivator-dependent receptor ligand assay. Molecular Endocrinology 1997;11(6):779–91.
[8] Evans RL, Reiser DJ. Role transitions for new clinical leaders in perinatal practice. Journal of Obstetric, Gynecologic & Neonatal Nursing 2004;33(3):355–61.
[9] Postic C, Girard J. Contribution of de novo fatty acid synthesis to hepatic steatosis and insulin resistance: lessons from genetically engineered mice. The Journal of Clinical Investigation 2008;118(3):829–38.
[10] López M, Nogueiras R, Tena-Sempere M, Diéguez C. Hypothalamic AMPK: a canonical regulator of whole-body energy balance. Nature Reviews Endocrinology 2016;12:421.
[11] Li Y-H, Luo J, Mosley Y-Yi C, Hedrick Victoria E, Paul Lake N, Chang J, Zhang G, Wang YK, Banko MR, Brunet A, et al. AMP-activated protein kinase directly phosphorylates and destabilizes hedgehog pathway transcription factor GLI1 in medulloblastoma. Cell Reports 2015;12(4):599–609.
[12] Foretz M, Viollet B. Regulation of hepatic metabolism by AMPK. Journal of Hepatology 2011;54(4):827–9.
[13] Ruderman N, Prentki M. AMP kinase and malonyl-CoA: targets for therapy of the metabolic syndrome. Nature Reviews Drug Discovery 2004;3:340.
[14] Chen G, Li H, Gao Y, Zhang L, Zhao Y. Flavored black ginseng exhibited antitumor activity via improving immune function and inducing apoptosis. Food & Function 2017;8(5):1880–9.
[15] Lee SR, Kim MR, Yon JM, Baek IJ, Park CG, Lee BJ, Yun YW, Nam SY. Black ginseng inhibits ethanol-induced teratogenesis in cultured mouse embryos through its effects on antioxidant activity. Toxicology in Vitro : An International Journal Published in Association with BIBRA 2009;23(1):47–52.
[16] Nam KY, Kim YS, Shon MY, Park JD. Recent advances in studies on chemical constituents and biological activities of Korean black ginseng(panax ginseng C. A. Meyer). Korean Journal of Pharmacognosy 2015;46(3):173–88.
[17] Bak MJ, Jeong WS, Kim KB. Detoxifying effect of fermented black ginseng on H2O2-induced oxidative stress in HepG2 cells. Int J Mol Med 2014;34(6):1516–22.
[18] Ha J, Shim YS, Seo D, Kim K, Ito M, Nakagawa H. Determination of 22 ginsenosides in ginseng products using ultra-high-performance liquid chromatography. Journal of Chromatographic Science 2013;51(4):355–60.
[19] Tominaga H, Ishiyama M, Ohseto F, Sasamoto K, Hamamoto T, Suzuki K, Watanabe M. A water-soluble tetrazolium salt useful for colorimetric cell viability assay. Analytical Communications 1999;36(2):47–50.
[20] Folch J, Lees M, Sloane Stanley GH. A simple method for the isolation and purification of total lipides from animal tissues. The Journal of Biological Chemistry 1957;226(1):497–509.
[21] Yoo JH, Liu Y, Kim HS. Hawthorn fruit extract elevates expression of Nrf2/HO-1 and improves lipid profiles in ovariectomized rats. Nutrients 2016;8(5).
[22] Ohkawa H, Ohishi N, Yagi K. Assay for lipid peroxides in animal tissues by thiobarbituric acid reaction. Analytical Biochemistry 1979;95(2):351–8.
[23] Sun BS, Gu LJ, Fang ZM, Wang CY, Wang Z, Lee MR, Li Z, Li JJ, Sung CK. Simultaneous quantification of 19 ginsenosides in black ginseng developed from Panax ginseng by HPLC-ELSD. Journal of Pharmaceutical and Biomedical Analysis 2009;50(1):15–22.
[24] Elshafay A, Tinh NX, Salman S, Shaheen YS, Othman EB, Elhady MT, Kansakar AR, Tran L, Van L, Hirayama K, et al. Ginsenoside Rk1 bioactivity: a systematic review. PeerJ 2017;5:e3993.
[25] He B, Chen P, Yang J, Yun Y, Zhang X, Yang R, Shen Z. Neuroprotective effect of 20(R)-ginsenoside Rg(3) against transient focal cerebral ischemia in rats. Neuroscience Letters 2012;526(2):106–11.
[26] Bae EA, Han MJ, Kim EJ, Kim DH. Transformation of ginseng saponins to ginsenoside Rh2 by acids and human intestinal bacteria and biological activities of their transformants. Archives of Pharmacal Research 2004;27(1):61–7.
[27] Yang XD, Yang YY, Ouyang DS, Yang GP. A review of biotransformation and pharmacology of ginsenoside compound K. Fitoterapia 2015;100:208–20.
[28] Lozano I, Van der Werf R, Bietiger W, Seyfritz E, Peronet C, Pinget M, Jeandidier N, Maillard E, Marchioni E, Sigrist S, et al. High-fructose and high-fat diet-induced disorders in rats: impact on diabetes risk, hepatic and vascular complications. Nutrition & Metabolism 2016;13:15.
[29] Chidambaram J, Carani Venkatraman A. Cissus quadrangularis stem alleviates insulin resistance, oxidative injury and fatty liver disease in rats fed high fat plus fructose diet. Food and Chemical Toxicology 2010;48(8):2021–9.
[30] Hu JN, Liu Z, Wang Z, Li XD, Zhang LX, Li W, Wang YP. Ameliorative effects and possible molecular mechanism of action of black ginseng (panax ginseng) on acetaminophen-mediated liver injury. Molecules (Basel, Switzerland) 2017;22(4).
[31] Jacome-Sosa MM, Parks EJ. Fatty acid sources and their fluxes as they contribute to plasma triglyceride concentrations and fatty liver in humans. Current Opinion in Lipidology 2014;25(3):213–20.
[32] Saba E, Jeon BR, Jeong DH, Lee K, Goo YK, Kim SH, Sung CK, Roh SS, Kim SD, Kim HK, et al. Black ginseng extract ameliorates hypercholesterolemia in rats. J Ginseng Res 2016;40(2):160–8.
[33] Sidhu GS, Oakenfull DG. A mechanism for the hypocholesterolaemic activity of saponins. The British Journal of Nutrition 1986;55(3):643–9.
[34] Lee MR, Kim BC, Kim R, Oh HI, Kim HK, Choi KJ, Sung CK. Anti-obesity effects of black ginseng extract in high fat diet-fed mice. Journal of Ginseng Research 2013;37(3):308–49.
[35] Gusdon AM, Song KX, Qu S. Nonalcoholic Fatty liver disease: pathogenesis and therapeutics from a mitochondria-centric perspective. Oxidative Medicine and Cellular Longevity 2014;2014:637027.
[36] Saw C, Yang AY, Cheng DC, Boyanapalli SSS, Su Z-Y, Khor TO, Gao S, Wang J, Jiang ZH, Kong AN. Pharmacodynamics of ginsenosides: antioxidant activities, activation of Nrf2 and potential synergistic effects of combinations. Chemical Research in Toxicology 2012;25(8):1574–80.
[37] Ucar F, Sezer S, Erdogan S, Akyol S, Armutcu F, Akyol O. The relationship between oxidative stress and nonalcoholic fatty liver disease: its effects on the development of nonalcoholic steatohepatitis. Redox Report : Communications in Free Radical Research 2013;18(4):127–33.

[38] Smith BK, Marcinko K, Desjardins EM, Lally JS, Ford RJ, Steinberg GR. Treatment of nonalcoholic fatty liver disease: role of AMPK. American Journal of Physiology-Endocrinology and Metabolism 2016;311(4):E730–40.

[39] Forbes-Hernández TY, Giampieri F, Gasparrini M, Afrin S, Mazzoni L, Cordero MD, Mezzetti B, Quiles JL, Battino M. Lipid accumulation in HepG2 cells is attenuated by strawberry extract through AMPK activation. Nutrients 2017;9(6):621.

[40] Kang HS, Cho HC, Lee JH, Oh GT, Koo SH, Park BH, Lee IK, Choi HS, Song DK, Im SS. Metformin stimulates IGFBP-2 gene expression through PPARalpha in diabetic states. Scientific Reports 2016;6:23665.

[41] Montagner A, Polizzi A, Fouché E, Ducheix S, Lippi Y, Lasserre F, Barquissau V, Régnier M, Lukowicz C, Benhamed F, et al. Liver PPARα is crucial for whole-body fatty acid homeostasis and is protective against NAFLD. Gut 2016;65(7):1202–14.

[42] McGarry JD, Brown NF. The mitochondrial carnitine palmitoyltransferase system — from concept to molecular analysis. European Journal of Biochemistry 1997;244(1):1–14.

[43] Gao X, Li K, Hui X, Kong X, Sweeney G, Wang Y, Xu A, Teng M, Liu P, Wu D. Carnitine palmitoyltransferase 1A prevents fatty acid-induced adipocyte dysfunction through suppression of c-Jun N-terminal kinase. Biochemical Journal 2011;435(3):723–32.